

## Modeling and Simulation of DC Power Electronics Systems Using Harmonic State Space (HSS) Method

Kwon, Jun Bum; Wang, Xiongfei; Bak, Claus Leth; Blaabjerg, Frede

*Published in:*

Proceedings of the 16th Annual IEEE Workshop on Control and Modeling for Power Electronics, COMPEL 2015

*DOI (link to publication from Publisher):*

[10.1109/COMPEL.2015.7236494](https://doi.org/10.1109/COMPEL.2015.7236494)

*Publication date:*

2015

*Document Version*

Accepted author manuscript, peer reviewed version

[Link to publication from Aalborg University](#)

*Citation for published version (APA):*

Kwon, J. B., Wang, X., Bak, C. L., & Blaabjerg, F. (2015). Modeling and Simulation of DC Power Electronics Systems Using Harmonic State Space (HSS) Method. In *Proceedings of the 16th Annual IEEE Workshop on Control and Modeling for Power Electronics, COMPEL 2015* IEEE Press.

<https://doi.org/10.1109/COMPEL.2015.7236494>

### General rights

Copyright and moral rights for the publications made accessible in the public portal are retained by the authors and/or other copyright owners and it is a condition of accessing publications that users recognise and abide by the legal requirements associated with these rights.

- Users may download and print one copy of any publication from the public portal for the purpose of private study or research.
- You may not further distribute the material or use it for any profit-making activity or commercial gain
- You may freely distribute the URL identifying the publication in the public portal -

### Take down policy

If you believe that this document breaches copyright please contact us at [vbn@aub.aau.dk](mailto:vbn@aub.aau.dk) providing details, and we will remove access to the work immediately and investigate your claim.



# Modeling and Simulation of DC Power Electronics Systems Using Harmonic State Space (HSS) Method

JunBum Kwon, Xiongfei Wang, Claus Leth Bak, Frede Blaabjerg  
Department of Energy Technology  
Aalborg University  
Aalborg, Denmark  
E-mail : {jbk, xwa, clb, fbl} @et.aau.dk

**Abstract**—For the efficiency and simplicity of electric systems, the dc based power electronics systems are widely used in variety applications such as electric vehicles, ships, aircrafts and also in homes. In these systems, there could be a number of dynamic interactions between loads and other dc-dc converters. Hence, in order to analyze these problems, simulations are required to consider such a complex system, which typically are time consuming. However, simulations in the time domain may increase the calculation time and computer memory. Even though several simplified approaches may be developed based on the state-space averaging and generalized averaging, these also have limitations to show the same results as with the non-linear time domain simulations. This paper presents a modeling and simulation method for a large dc power electronic system by using Harmonic State Space (HSS) modeling. Through this method, the required computation time and CPU memory for large dc power electronics systems can be reduced. Besides, the achieved results show the same results as with the non-linear time domain simulation, but with the faster simulation time which is beneficial in a large network.

**Keywords**—Harmonic State Space Modeling, DC distribution network, Harmonic instability

## I. INTRODUCTION

Due to the advantages like high energy efficiency, lower line losses, and also a simpler structure, the dc power electronics systems are becoming more used in a variety of application. For instance, electric ship, aircraft, home network, medical systems, and dc micro-grid are important applications [1-3]. In these dc power electronics systems, the interaction can happen due to the connection to other converters and loads such as constant power loads [4]. As a result, the variety of these interactions can be increased as the complexity of the connection is increasing. Hence, a proper simulation tool is required to study these interactions.

However, there are many difficulties in the time-domain simulation of large complex systems. The transient and steady-state simulation using switching models of power electronic converters require a large computer memory and long-term simulation time due to a time-step variation. To simplify the models and reduce the simulation time, the State-Space Averaging (SSAV) method was introduced [5]. However, if the system is defined as a large signal to analyze the system level studies, the SSAV can not be used anymore. Furthermore, fast transient dynamics can not be applied by the

SSAV. A Generalized state-space Averaging (GAV) method was also considered for the implementation of large power electronics systems in order to model and include important harmonics into the simulations [2, 6, 7]. However, it can not include the interaction between the non-linear components. Besides, due to the simplicity of harmonics components, it ignores also the possibility of modelling the interaction with other harmonics in a large network simulation.

The harmonics in the dc systems are new challenges to be analyzed with ac distribution systems because the dc is originally from ac-dc converters. To overcome this challenge and to show other harmonic impedance couplings, a Harmonic State Space (HSS) modeling method [8] is introduced in the power system studies. Based on the theory of Harmonic Domain (HD) [9], Extended Harmonic Domain (EHD) [10], and Harmonic Transfer Function (HTF) [11], the HSS modeling method is developed in order to analyze the harmonic coupling and stability with additional harmonic impedances for complex systems. Before it was used in power system analysis as well it has been widely used in determining mechanical resonances of wind turbine blades, blade analysis of helicopters and also structural resonance analysis of bridges to identify the uncertain characteristics, which can not be found by the conventional LTI analysis approach [12].

This paper proposes a new model for dc power electronics systems by means of the HSS modeling method. First, the modeling procedures for dc-dc converters such as: buck, boost and buck-boost are explained briefly. Second, the multi-parallel connected dc-dc converters are implemented based on the single dc-dc converter modeling results. Third, both the steady-state and dynamic characteristics among the converters are simulated by using the HSS method. The analyzed results are verified by the time-domain and the frequency-domain simulations.

## II. HSS MODELING METHOD FOR DC POWER ELECTRONICS SYSTEMS

### A. Review of HSS modeling

The HSS modeling method is originally introduced to include time-varying points of a linearized model. The Linear Time-Varying (LTV) model is practically a non-linear model because of the varying characteristic of the system parameters. Hence, the model is difficult to be solved at a specific

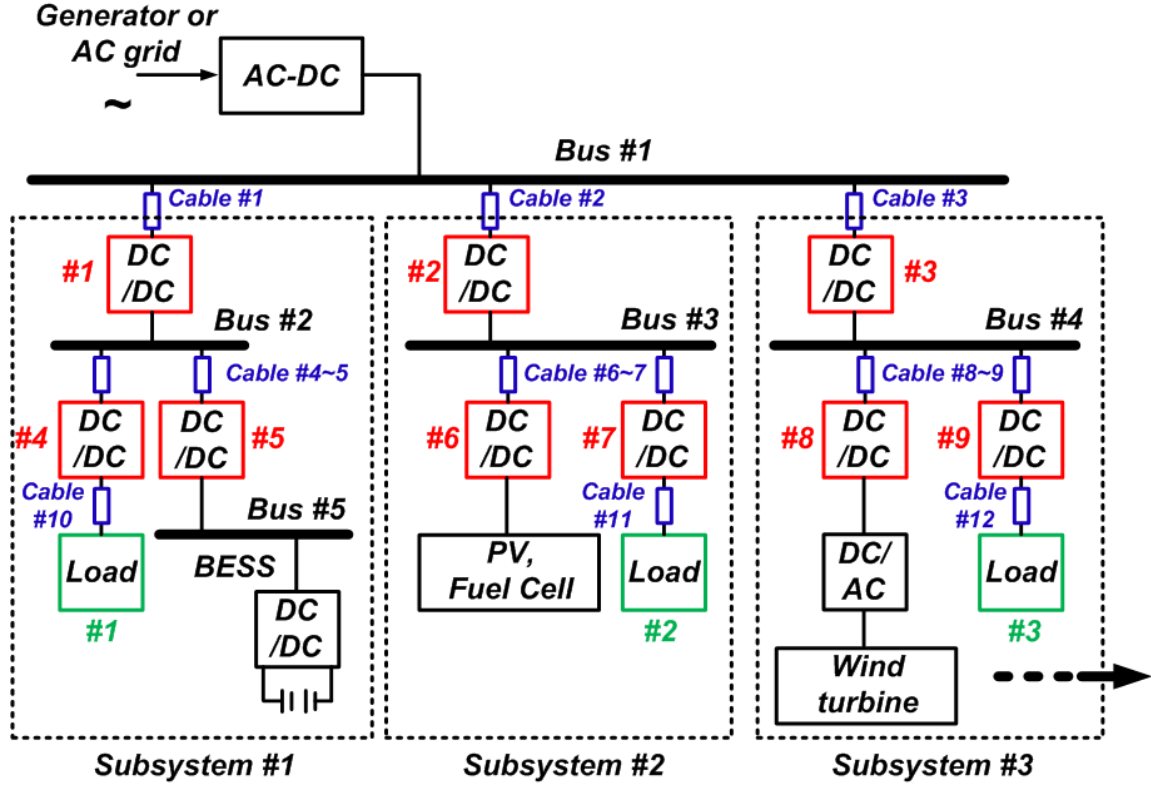


Fig. 1. Multi-converter dc power electronics system (9 dc-dc converters (#1~#9), 3 dc loads (#1~#3)).  
BESS (=Battery Energy Storage System)

operating point as like in the Linear Time Invariant (LTI) model. However, if all signals are assumed to be varying periodically, it is possible to linearize the model by means of Fourier series. Based on these assumptions and definitions, the HSS model can have a format as shown in (1), where  $X_n$  is the harmonic state matrix,  $Y_n$  is the output harmonic matrix,  $U_m$  is input harmonic matrix and  $A_{n-m}$  is the harmonic system matrix driven by the Linear Time-varying Periodically (LTP) theory [12].  $B_{n-m}$ ,  $C_{n-m}$ ,  $D_{n-m}$  are also harmonic state matrixes, which are dependent on the number of input and output. All the matrix sizes are dependent on the number of harmonics considered in the HSS modeling procedure.

$$\begin{aligned} (s + jm\omega_0)X_n &= \sum_{m=-\infty}^{\infty} A_{n-m}X_m + \sum_{m=-\infty}^{\infty} B_{n-m}U_m \\ Y_n &= \sum_{m=-\infty}^{\infty} C_{n-m}X_m + \sum_{m=-\infty}^{\infty} D_{n-m}U_m \end{aligned} \quad (1)$$

Each time-varying harmonic vector ( $X$ ,  $U$ ,  $Y$ ) can be transformed into the time domain by using (2).

$$x(t) = \Gamma(t)X \quad (2)$$

where,

$$\begin{aligned} \Gamma(t) &= [e^{-jh\omega_0 t} \dots e^{-j2\omega_0 t}, e^{-j\omega_0 t}, 1, e^{j\omega_0 t}, e^{j2\omega_0 t} \dots e^{jh\omega_0 t}] \\ X &= [X_{-h}(t) \dots X_{-1}(t) X_0(t) X_1(t) \dots X_h(t)]^T \end{aligned}$$

### B. Topology modeling

Based on the modeling procedure, all components can be modeled into the HSS model. A multi-converter dc power electronics system is shown in Fig. 1, where the dc-dc

converters (#1~#9) and dc-loads (#1~#3) are only considered in this paper. The other related converters such as bi-directional dc-dc converter and ac-dc converter are assumed as constant dc-voltage / current sources. Based on (1), three principal converters (Buck, Boost, Buck-Boost) are modeled according to the procedure described in [12, 13]. Even though there are more various kinds of circuits and thereby models such as: full bridge type, inter-leaved converter, fly-back converter, these topologies are also developed from three principal models.

According to (1)-(2), the topology of 3-converters can be done as shown in Table I and (4)-(6), where “ $N$ ” is a dynamic harmonic vector as shown in (3), “diag( $\cdot$ )” means the diagonal matrix and “ $Z$ ” means the zero-matrix.

$$N = \text{diag}[-jk\omega_0 \dots -j\omega_0, 0, j\omega_0, \dots jk\omega_0] \quad (3)$$

In the case of a switching element, the harmonic components should be transformed into the Toeplitz matrix ( $\Gamma(\cdot)$ ) in order to perform a convolution. Furthermore, it is noted that the switching vector ( $\Gamma(\text{SW}(t))$ ) will be updated from the controller in every state change. In addition, the number of harmonic vectors decides the accuracy of the modeling results. Hence, the optimized selection of both the fundamental frequency and the number of harmonics vector is an important criteria to do a fast and accurate simulation. In this paper, the fundamental frequency ( $f_0$ ) is selected to be 500 Hz and the number of harmonics considered is of the 20<sup>th</sup> order harmonics for each component.

Table I. Circuit diagram and HSS modeling of dc-dc converters for use in dc-grid.  
(a) Buck converter, (b) Boost converter, (c) Buck-boost converter, where Z is zero matrix.

<p>(a)</p>	$\begin{bmatrix} \dot{I}_L(t) \\ \dot{V}_{out}(t) \end{bmatrix} = \begin{bmatrix} -N & \text{diag}(-\frac{1}{L}) \\ \text{diag}(\frac{1}{C_{dc}}) & -N \end{bmatrix} \begin{bmatrix} I_L(t) \\ V_{out}(t) \end{bmatrix} + \begin{bmatrix} \frac{\Gamma(SW(t))}{L} & Z \\ Z & \text{diag}(-\frac{1}{C_{dc}}) \end{bmatrix} \begin{bmatrix} V_{in}(t) \\ I_{Load}(t) \end{bmatrix} \quad (4)$
<p>(b)</p>	$\begin{bmatrix} \dot{I}_L(t) \\ \dot{V}_{out}(t) \end{bmatrix} = \begin{bmatrix} -N & -\Gamma(1-SW(t)) \\ \frac{\Gamma(1-SW(t))}{C_{dc}} & -N \end{bmatrix} \begin{bmatrix} I_L(t) \\ V_{out}(t) \end{bmatrix} + \begin{bmatrix} \text{diag}(\frac{1}{L}) & Z \\ Z & \text{diag}(-\frac{1}{C_{dc}}) \end{bmatrix} \begin{bmatrix} V_{in}(t) \\ I_{Load}(t) \end{bmatrix} \quad (5)$
<p>(c)</p>	$\begin{bmatrix} \dot{I}_L(t) \\ \dot{V}_{out}(t) \end{bmatrix} = \begin{bmatrix} -N & -\frac{\Gamma(1-SW(t))}{L} \\ \frac{\Gamma(1-SW(t))}{C_{dc}} & -N \end{bmatrix} \begin{bmatrix} I_L(t) \\ V_{out}(t) \end{bmatrix} + \begin{bmatrix} \frac{\Gamma(SW(t))}{L} & Z \\ Z & \text{diag}(-\frac{1}{C_{dc}}) \end{bmatrix} \begin{bmatrix} V_{in}(t) \\ I_{Load}(t) \end{bmatrix} \quad (6)$

The expressions of the harmonics vector are given in Fig. 2, where the buck converter is used as an example to explain how the harmonics vectors are updated to the other components during calculation. The harmonics vectors of the other converters can also be transferred to their own components in a similar way. The small letter in Table I. (a)~(c) means the time domain signal. The capital letters in Fig. 2 and Table I. (4)~(6) stand for the harmonic coefficient component, which are derived from the Fourier series.

Each block has its input (U) and output (Y) harmonic vector as shown in Fig. 2. In the case of a buck converter model, the module is divided into three blocks, namely, “L-R Circuit”, “R-C Circuit”, “Switch Circuit”. The time domain switching function is reorganized into a Toeplitz ( $\Gamma$ ) [14] matrix in order to perform a convolution as shown in Fig. 2 (SW). First, the input dc voltage harmonic vector ( $V_{in}$ ) is convoluted with switching Toeplitz matrix (SW). The results

can be the input vector ( $V_1$ ) of the “L-R circuit. Another input vector ( $V_{out}$ ) of the “L-R Circuit” can be derived from the “R-C Circuit”. The result ( $I_L$ ) of “L-R Circuit” is the input vector of “R-C Circuit”, where the “R-C Circuit” is including the load (R) information and this can be changed into the current / voltage source. The inductor current ( $I_L$ ) vector can also be convoluted with the switching vector (SW) in order to calculate the input vector of the input current harmonic ( $I_{in}$ ). Conclusively, all input, output, and state harmonics vector are iteratively updated as shown in Fig. 2.

By using each achieved model, the simulation of multiple dc-dc converters is possible. A similar approach using the Generalized Averaging (GAV) [2] is introduced in order to reduce the simulation time as well as the complexity. However, the GAV normally adapts a relatively large harmonics than other harmonics. Hence, it is difficult to see the harmonics interaction, which is happened by other harmonics. The

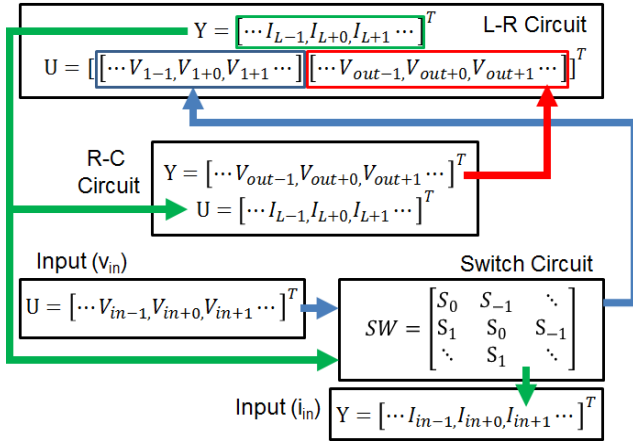


Fig. 2. Block diagram of the harmonics vector flow for calculation of buck converter.

importance of this characteristic is noticeable, when the dc-dc converters are connected with an ac-dc converter interface such as: wind turbine, photovoltaics, micro turbine and ac-loads. Besides, the investigation and calculation of how the harmonics are related is not necessary, because of the modularity of the components as shown in Fig. 2 and Table I.

### C. Controller modeling

In this paper, the dc-output is only considered as a target to control the dc-dc converter in order to take into account the controller performance in the dc-dc converter model. However, in order to account for the dynamics, which is the case by the nonlinear switching, the controller should also be linearized as the case of the linearized topology model in Fig. 2.

The different procedures can be compared with the time-domain simulation. In the calculation procedure of the time-domain results, the product of two time domain signals can be represented as shown in (7).

$$\text{out}(t) = u(t) \cdot \text{in}(t) \quad (7)$$

where,  $\text{in}(t)$ ,  $\text{out}(t)$  are the input and output signals, respectively and  $u(t)$  is the time signals to change the formulation of the input. For instance,  $u(t)$  can be a switching signal ( $sw(t)$ ) or a nonlinear component like an inductor. On the contrary to (7), the linearized harmonics vector can be considered in the HSS model in order to reflect the variation of the nonlinear time-varying components ( $u(t)$ ) as shown in (8).

$$\Delta \text{OUT}(t) = U_{\text{base}} \cdot \Delta \text{IN}(t) + \Delta U(t) \cdot \text{IN}_{\text{base}} \quad (8)$$

where, the  $U_{\text{base}}$ ,  $\text{IN}_{\text{base}}$  are the harmonics vector of the previous state and the  $\Delta \text{IN}(t)$ ,  $\Delta U(t)$  are the small variation of the harmonics vector ( $\text{IN}(t)$ ,  $U(t)$ ). The division of two time domain signals can be linearized by means of the partial differentiation as shown in (7) and (8).

The block diagram for the generalized dc-voltage controller is shown in Fig. 3, where the signals with small letters are the time domain signals and the signals with capital mean the harmonics vector, which is including the 20<sup>th</sup> order

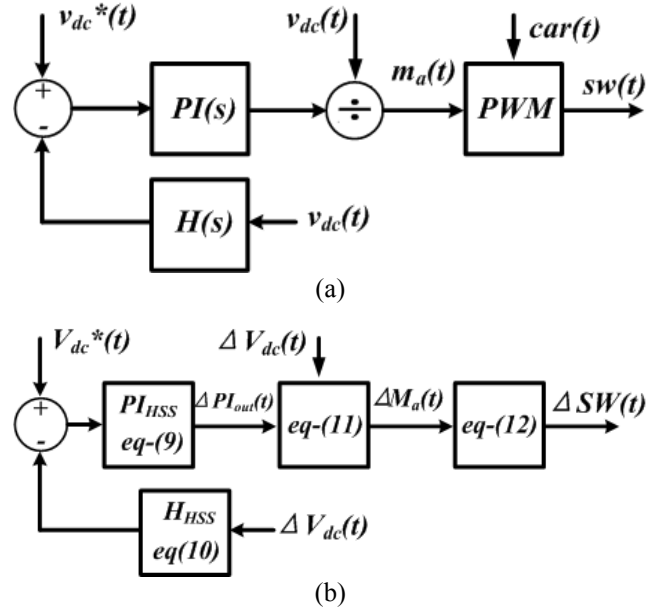


Fig. 3. Block diagram of a generalized controller for the dc-dc converter. (a) Nonlinear simulation model for the time domain signals, (b) Linearized simulation model for the HSS model, where the capital means the harmonic vector

harmonics in the vector. According to the procedure given in (7) and (8), the nonlinear simulation model in Fig. 3-(a) can be linearized into the HSS model as shown in Fig. 3-(b). The detailed equations derived from the linearization are shown in (9)-(12).

$$\text{PI}_{\text{HSS}} = \begin{bmatrix} \text{PI}(s - jh\omega_0) & & \\ & \ddots & \\ & & \text{PI}(s) \\ & & & \ddots \\ & & & & \text{PI}(s + jh\omega_0) \end{bmatrix} \quad (9)$$

where,  $\text{PI}(s) = K_p + K_i/s$ ,  $K_p$  is the proportional gain,  $K_i$  is the integrator gain and  $\text{PI}_{\text{HSS}}$  is the HSS format of  $\text{PI}(s)$ .

$$\text{H}_{\text{HSS}} = \begin{bmatrix} H(s - jh\omega_0) & & \\ & \ddots & \\ & & H(s) \\ & & & \ddots \\ & & & & H(s + jh\omega_0) \end{bmatrix} \quad (10)$$

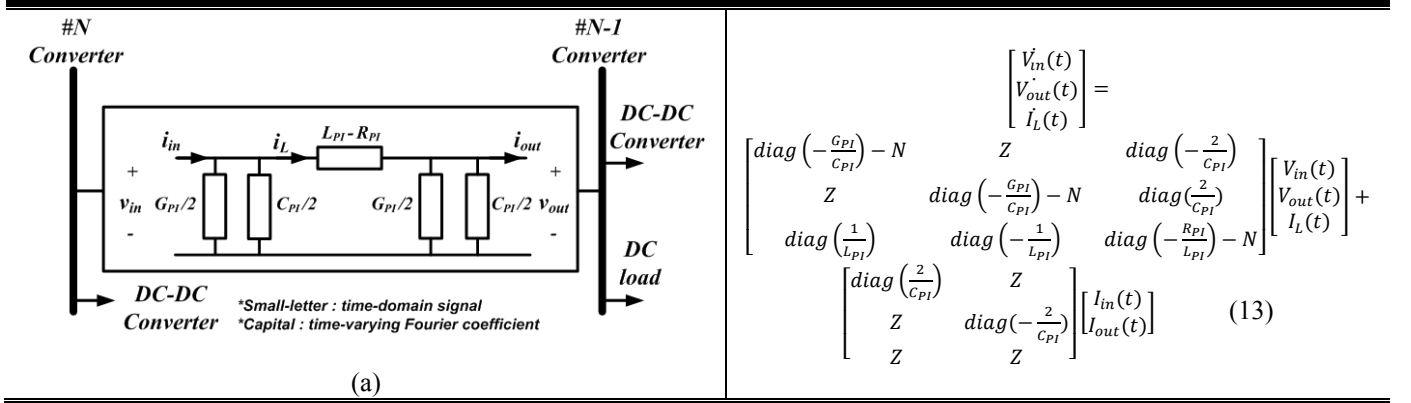
where,  $H(s) = 1/(s \cdot K_{\text{lpf}} + 1)$  with  $K_{\text{lpf}}$  as the low pass filter bandwidth and  $\text{H}_{\text{HSS}}$  is the HSS format of  $H(s)$ .

$$\Delta M_a(t) = -\frac{\text{PI}_{\text{out}}^b}{(v_{dc}^b) \Gamma(v_{dc}^b)} \Delta V_{dc}(t) + \frac{1}{v_{dc}^b} \Delta \text{PI}_{\text{out}}(t) \quad (11)$$

where, the  $v_{dc}^b$ ,  $\text{PI}_{\text{out}}^b$  are the previous state values and the  $\Delta V_{dc}(t)$ ,  $\Delta \text{PI}_{\text{out}}(t)$ ,  $\Delta M_a(t)$  are the updated states of the dc voltage, the output of PI controller and the modulation index.

$$\Delta \text{SW}(t) = \Gamma(\text{SW}_n - \text{SW}_{n-1}) \Delta M_a(t) \quad (12)$$

Table II. Circuit diagram and HSS modeling of low-voltage dc cable  
(a) Circuit diagram of Cable model (PI section), where Z is the zero matrix



where, the  $SW_n, SW_{n-1}$  are the present and previous status of the PWM harmonics vector.

The updated harmonics vectors in Fig. 3-(b) are continuously transferred to the state vector of the dc-dc converter in order to update the status. The linearized dc-voltage controller is used in the 3 different topologies with different controller gain.

#### D. Low voltage dc-cable modeling

In order to consider the interaction, which can happen by a cable connection, a low voltage dc-cable is also modeled. Instead of using a simple inductance or resistance model, the PI-section model is taken into account according to the length of the cable. The derived result is shown in Fig. 4, where the HSS modeling theory ((1) ~ (3)) is also used to include the harmonics in the model and  $G_{PI}, C_{PI}, L_{PI}, R_{PI}$  are conductance, capacitance, inductance and resistance of the PI-section cable model. In addition, the acronyms and subscripts used in (13) have also the same meaning as (4) ~ (6). The obtained cable model is combined with other converters and loads as shown in Fig. 1. (Cable #1 ~ Cable #12).

An ac-cable is considered in the dc-grid system to adapt practical data for simulations. The used cable data are as follows [15]:

- Current Rating : 200 A
- Cable Type : 3-Conductor A1-PVC 185 mm<sup>2</sup>
- Resistance : 0.152 mΩ/meter
- Inductance : 0.237 uH/meter
- Capacitance : 2 pF/meter (assumed)
- Cable length : 1000 m (Cable #1~Cable #12)

The conductance is not taken into account in the parameters and the capacitance is determined as the assumed values. However, the effect of the capacitance can be neglected because the dc system does not need to consider the reactive power driven by the parasitic capacitance of the cable.

### III. HSS SIMULATION RESULTS

To validate the modeling and analysis results of the dc power electronics system, MATLAB and PLECS are used for

time and frequency domain simulations to illustrate the two different assessment methods. All the simulations have been performed using the i7-4800MQ CPU (2.7 GHz). The presented dc-dc converter models are used to validate the dc power electronics systems.

#### A. Simulation parameters

In order to show the switching ripple in the simulation, the switching frequency of each dc-dc converter is assumed to be 5 kHz. The Bus #1 in Fig. 1 is assumed to be 200 V<sub>dc</sub>. Based on the dc-voltage of the main bus (Bus #1), the dc voltage is boosted by using the dc-dc converters (#1 ~ #3). The buck converters (#4, #9) are considered to step down the voltage for the loads (#1, #3). The buck-boost converters (#5, #6) are considered to control the dc-voltage in order to manage a time varying dc-voltage (BESS, PV, Fuel Cell). In addition, the boost converters (#7, #8) are taken into account to step up the voltage for the load and for a wind turbine as shown in Fig. 1. For the simplicity of the simulation model, the outputs of PV, BESS and wind turbine are assumed to have a constant dc voltage. The resistive loads are only considered for the simulations. However, the proposed simulation model can be extended in order to connect to the constant voltage loads, constant power loads and other RLC loads.

#### B. HSS module connection

In order to connect the developed module in the previous section, it is required to link both the input and output harmonics vector into a final model. Three examples are shown in Fig. 4 to explain how the HSS module can be connected with others, where the capital means the harmonics vector as given in (2).

The final input and output vectors of each dc-dc converters can be defined by the dc-voltage reference ( $V_{dc}^*$ ), the input voltage ( $V_{in}$ ) and the output load current ( $I_{load}$ ), in addition the output voltage ( $V_{out}$ ) and input current ( $I_{in}$ ) are the output harmonics vector. The cables and loads can also be similarly defined.

The cable and single converters can be connected as shown in Fig. 4-(a), where the output voltage of the cable can be linked to the input voltage of the dc-dc converters and the input

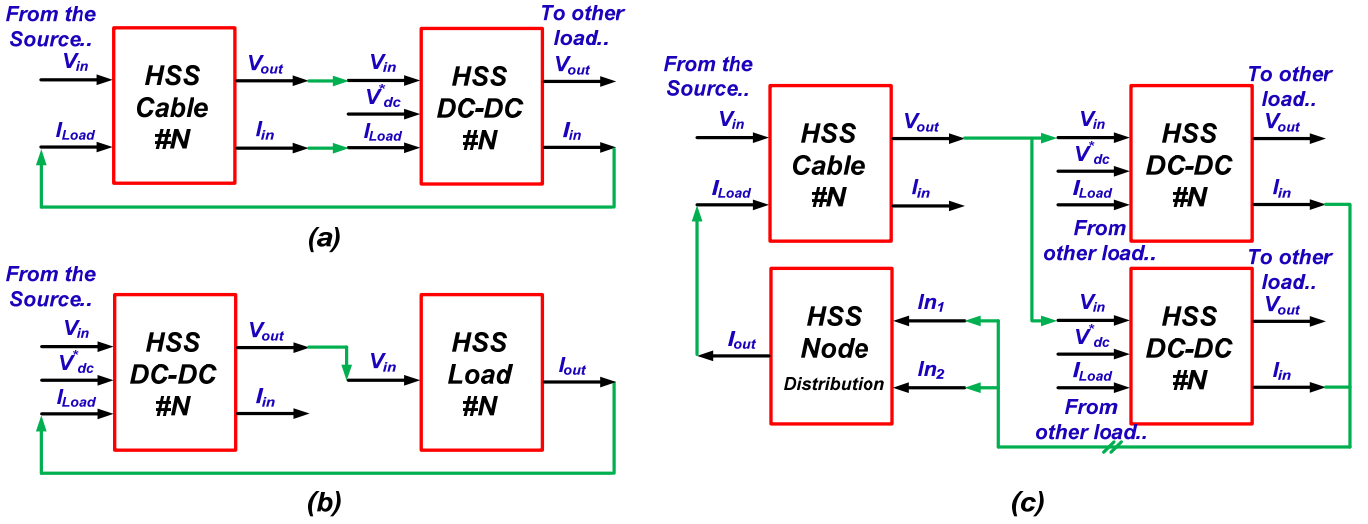


Fig. 4. Block diagram for the connection of each HSS module into a full simulation cases.

(a) dc-dc converter connection with single cable, (b) dc-dc converter connection with single load, (c) 2- parallel connected dc-dc converters connected with a single input cable

current vector of dc-dc converters is connected to the output harmonics vector of the cable. The connection with the dc-dc converter and load can be done as shown in Fig. 4-(b). However, in the case of parallel connection of converters or cables, a node distribution matrix ( $Dist_{node}$ ) is required to divide or to combine the multi current /voltage signals, simultaneously, as shown in Fig. 4-(c). The formulation to do this can be defined as (14).

$$Dist_{node} = [eye(k)_1, eye(k)_2, \dots, eye(k)_n] \quad (14)$$

where, the  $eye(\cdot)$  means the identity matrix and the size of matrix is dependent on the number harmonics ( $k$ ). Additionally, the “ $n$ ” means the number of nodes to be added into one node.

### C. Simulation (Steady-state /dynamic)

Based on the assumed parameters, the simulations and comparisons are derived as shown in Fig. 5. The harmonic vector obtained from (1) can be converted into the time domain by rotating with the harmonic frequency. The summation of each harmonics into a time domain signal is shown in Fig 5. The results show that the HSS simulations are matched well with the non-linear time domain simulations (PLECS) as shown in Fig 5. Conclusively, the HSS is a frequency domain model, which can derive the same results with a non-linear time domain simulation. This means the HSS can show both the steady-state and the dynamic performance, which can not be seen in LTI model, since the LTI model can only show a single sinusoidal input and the output characteristic. However, the LTP model can show multiple frequency output characteristic from a single sinusoidal input and show how the harmonic is coupled, attenuated and canceled with each other.

The simulation results are tested with two cases, a transient state from the starting point and the dynamic behavior from steady-state. Besides that, the accuracy of the simulation result

is also discussed with the comparison. The constant dc voltage ( $200 V_{dc}$ ) is stepped down to  $150 V_{dc}$  as shown in Fig. 5-(a). The main dc bus (Bus #1) is converted into  $500 V_{dc}$  through a boost converter as shown in Fig. 5-(b). The  $500 V_{dc}$  is also converted into  $250 V_{dc}$  by means of the buck-boost converter. The results show well the transient state from the starting point and the convergence into the steady state.

Furthermore, the dynamic response of the buck and boost converters during the steady-state, which happens when connecting the other load converters (@  $t=0.1$ ), shows the same results with the nonlinear time domain simulation as shown in Fig. 5-(c). According to the increased load, the output voltage converges to steady state and the load current increasing. Also, the output dc-voltage is tracking the reference voltage again as shown in Fig. 5-(d), even if the input dc voltage is changed. The input current is increased to keep the same output power during the operation.

Compared to the nonlinear time-domain simulation and the other modeling methods, the accuracy of the simulation depends on the number of harmonics and the precision of the Fourier series. Comparing the results show in Fig. 6-(a), (b), the precision can be increased as the number of harmonics increase. It provides also the possibility to see how the harmonics are coupled in one domain. However, the calculation time will be increased due to the size of the matrix.

In a short time simulation of a single converter, the nonlinear time-domain simulation is much faster than the HSS model ( $h=20$ ). However, the HSS model has similar performance, when the fundamental frequency is defined as the switching frequency and the number of harmonics is defined as a small number ( $h=3$ ). Furthermore, in this case, the HSS model has more advantages as the number of circuits increase. Also, the calculation time of the long term HSS simulation is shorter than the nonlinear time domain simulation.



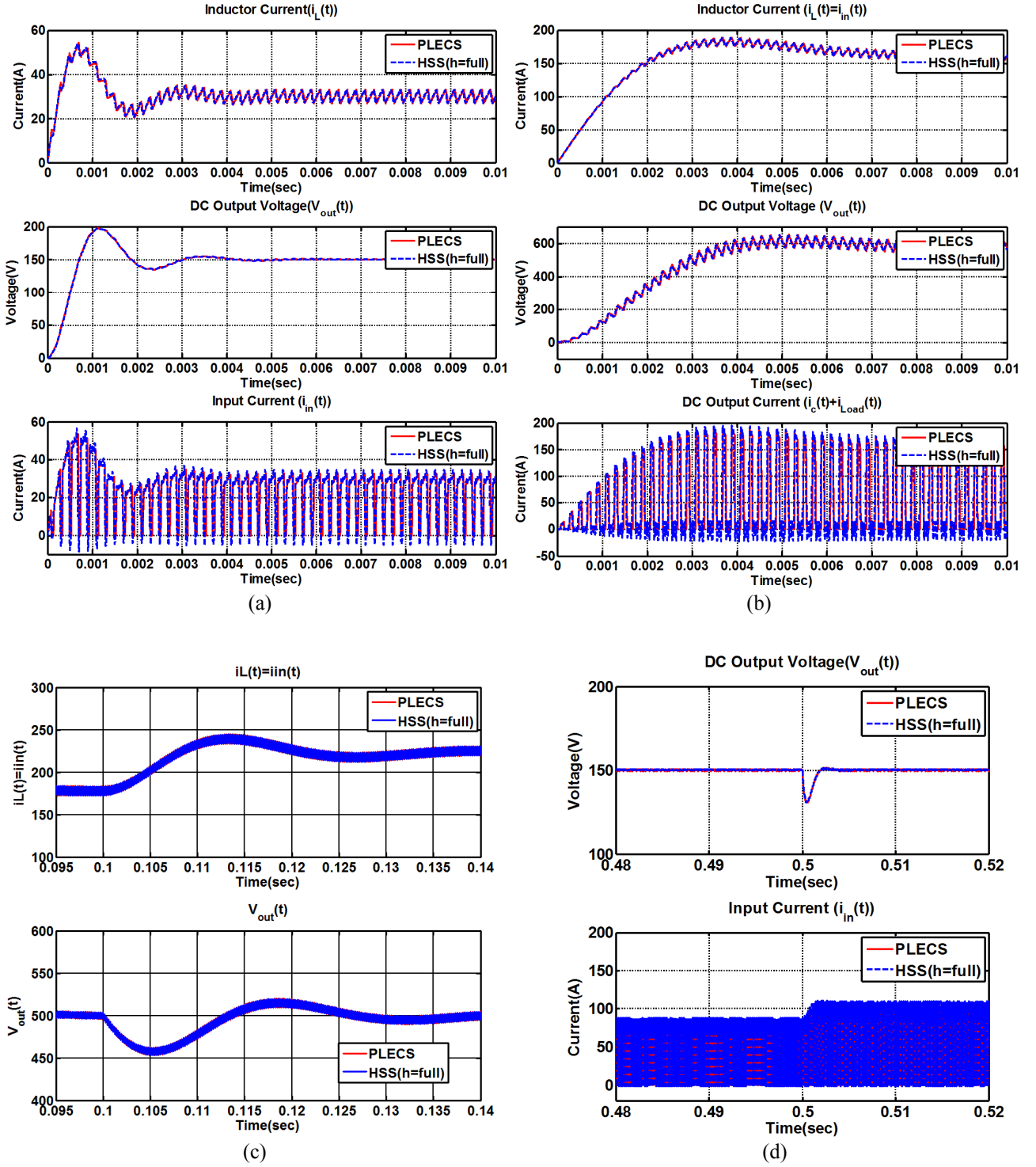


Fig. 5. Comparison of simulation results using the PLECS and HSS modeling (a) buck converter in Table I-(a), (b) boost converter in Table I-(b), (c) 20% dc-load (load converters) step of boost converter #5 at  $t=0.1$  ( $i_L(t)$ =inductor current,  $v_{out}(t)$ =dc output voltage), (d) 10% input-voltage reduction of buck converter #4 at  $t=0.5$  ( $i_{in}(t)$ =input current,  $v_{out}(t)$ =dc output voltage)

#### IV. CONCLUSION

This paper presents the modeling and simulation of dc power electronics systems by using an HSS modeling

approach. Each component as well as the dc-dc converters are modularized in order to connect them with other models. The selected converters are analyzed and validated by the proposed method. To verify the validity of the HSS model, the HSS

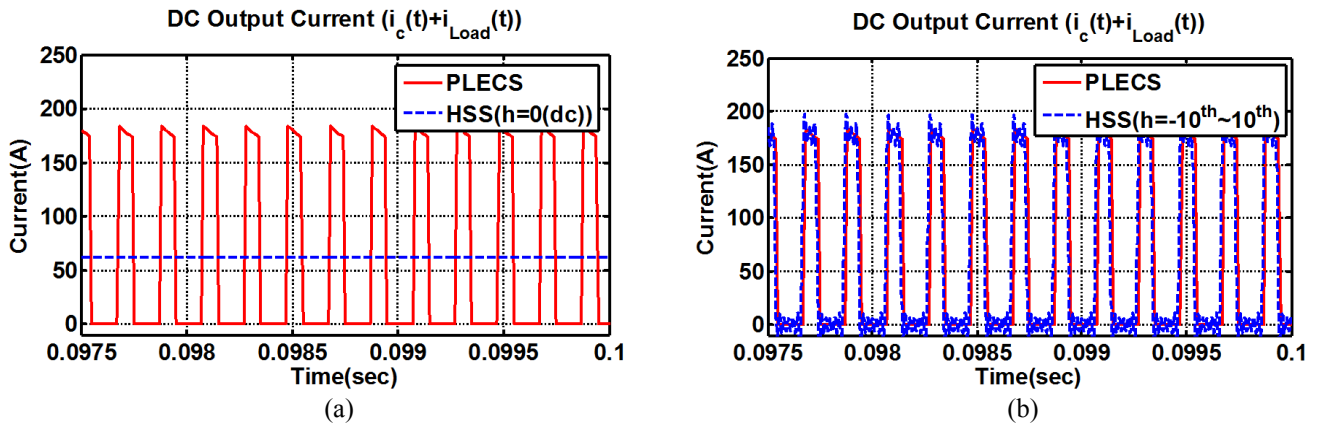


Fig. 6. Comparison of simulation precision according to the number of harmonics ( $i_c(t)$ =capacitor current,  $i_{Load}(t)$ =output load current), (a) Comparison of PLECS and HSS ( $h=0(dc)$ ), (b) Comparison of PLECS and HSS ( $h=-10^{th} \sim 10^{th}$ ).

simulation results are compared with the non-linear time domain simulation. In addition, the interaction between the source of the power converters and load power converters is also analyzed. The overall results derived from the HSS model show exactly the same performance, which means the transfer function derived from HSS model has more accurate characteristic than the conventional modeling method e.g., SSAV or GAV. Furthermore, the model proposed in this paper can include various harmonics, where it can be used for the analysis of harmonic interactions, the design of the controller or the stability assessment, which can not be found in the LTI model.

#### ACKNOWLEDGMENT

This work was supported by European Research Council under the European Union's Seventh Framework Program (FP/2007-2013)/ERC Grant Agreement n. [321149-Harmony].

#### REFERENCES

- [1] K. J. Karimi, A. Booker, and A. Mong, "Modeling, simulation, and verification of large DC power electronics systems," in *Proc. of IEEE PESC*, 1996, pp. 1731-1737 vol.2.
- [2] A. Emadi, "Modeling and analysis of multiconverter DC power electronic systems using the generalized state-space averaging method," *IEEE Trans. Ind. Electron.*, vol. 51, pp. 661-668, 2004.
- [3] X. Wang, F. Blaabjerg, and W. Weimin, "Modeling and Analysis of Harmonic Stability in an AC Power-Electronics-Based Power System," *IEEE Trans. on Power Electron.*, vol. 29, pp. 6421-6432, 2014.
- [4] R. D. Middlebrook, "Small-signal modeling of pulse-width modulated switched-mode power converters," *Proc. of IEEE*, vol. 76, pp. 343-354, 1988.
- [5] P. T. Krein, J. Bentsman, R. M. Bass, and B. C. Lesieutre, "On the use of averaging for the analysis of power electronic systems," *IEEE Trans. Power Electron.*, vol. 5, pp. 182-190, 1990.
- [6] S. R. Sanders, J. M. Noworolski, X. Z. Liu, and G. C. Verghese, "Generalized averaging method for power conversion circuits," *IEEE Trans. Power Electron.*, vol. 6, pp. 251-259, 1991.
- [7] A. Emadi, "Modeling of power electronic loads in AC distribution systems using the generalized State-space averaging method," *IEEE Trans. Ind. Electron.*, vol. 51, pp. 992-1000, 2004.
- [8] M. S. P. Hwang and A. R. Wood, "A new modelling framework for power supply networks with converter based loads and generators - the Harmonic State-Space," in *Proc. of IEEE POWERCON*, 2012, pp. 1-6.
- [9] J. Arrillaga and N. R. Watson, "The Harmonic Domain revisited," in *Proc. of IEEE ICHQP*, 2008, pp. 1-9.
- [10] B. Vyakaranam, M. Madrigal, F. E. Villaseca, and R. Rarick, "Dynamic harmonic evolution in FACTS via the extended harmonic domain method," in *Proc. of IEEE PECEI*, 2010, pp. 29-38.
- [11] E. Mollerstedt and B. Bernhardsson, "Out of control because of harmonics-an analysis of the harmonic response of an inverter locomotive," *IEEE Trans. on Control Sys.*, vol. 20, pp. 70-81, 2000.
- [12] N. M. Wereley and S. R. Hall, "Linear Time Periodic Systems: Transfer Function, Poles, Transmission Zeroes and Directional Properties," in *Proc. of IEEE ACC*, 1991, pp. 1179-1184.
- [13] K. JunBum, W. Xiongfei, C. L. Bak, and F. Blaabjerg, "Harmonic interaction analysis in grid connected converter using Harmonic State Space (HSS) modeling," in *Proc. of IEEE APEC 2015*, 2015, pp. 1779-1786.
- [14] J. R. C. Orillaza and A. R. Wood, "Harmonic State-Space Model of a Controlled TCR," *IEEE Trans. Power Deliv.*, vol. 28, pp. 197-205, 2013.
- [15] S. Anand and B. G. Fernandes, "Reduced-Order Model and Stability Analysis of Low-Voltage DC Microgrid," *IEEE Trans. Ind Electron.*, vol. 60, pp. 5040-5049, 2013.